

Super Cyclone Boosters in the Northwest Pacific Ocean

I-I Lin, Chun-Chieh Wu, and Iam-Fei Pun

Department of Atmospheric Sciences, National Taiwan University, Taipei, Taiwan

Submitted to the *Bulletin of the American Meteorological Society*

October 13, 2005

Abstract

Most of the world's most powerful tropical cyclones occur in the Northwest Pacific Ocean. How these category-five "super cyclones" obtain their extraordinary strength remains a mystery. Although the ensemble of cyclone tracks span over the entire Northwest Pacific Ocean, they apparently intensify only across a confined zone. Here we combine in-situ measurements, remote sensing, and numerical experiments to show that the intensification zone is delimited by an abundance of warm ocean eddies and by the thickest belt of warm subtropical gyre water. We suggest that the robust structure of these warm waters effectively counteracts cyclone's self-induced cooling that otherwise restrains a tropical cyclone from intensification. Understanding of boosters in other ocean basins, such as those which may have fuelled the recent Super hurricane Katrina, serves to instil greater preparedness and mitigation of disaster resulted from super cyclones.

Category-5 (1-minute averaged wind speed > 135 kt) super cyclones, like Hurricane Katrina (2005) and Supertyphoon Maemi (2003), are the most intense and destructive storm system on earth. In spite of their huge impact, current understanding of why these cyclones can reach such extraordinary intensity is still limited (Emanuel, 2000a; Goni and Trinanes, 2003; Wang and Wu, 2004; Emanuel, 2005). Most of these super cyclones are found in the Northwest Pacific Ocean. One long-specified but unanswered question is that though the tracks of super cyclones may cover the entire Northwest Pacific Ocean, the critical intensification process, i.e., from the modest category-1 (1-minute averaged wind speed 64-82 kt) to the super-strength category-5, is confined only in a well-defined area over the ocean (Holliday and Thompson, 1979). As illustrated in Fig. 1a, the intensification for all of the 90 super cyclones¹ occurring during the tropical

cyclone season (May-October) from 1960-2005 took place only within the zone of 121-170° E, 9-25° N.

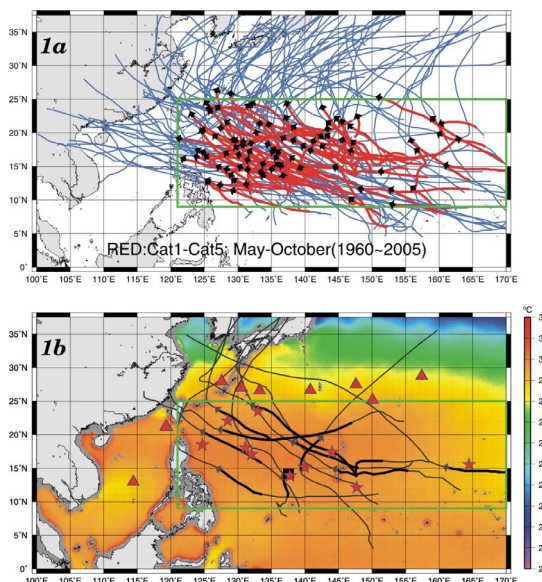


Figure 1: (a): The location of intensification (from category-1 to 5, shown in red segment with arrow) for the 90 super cyclones occurring in the Northwest Pacific Ocean during the May-October typhoon season in 1960-2005. The rest of the tracks are depicted in blue while the green box defines the intensification zone (121-170° E, 9-25° N). (b): Same as in (a), showing the full tracks (in grey) and intensification track segments (in black with arrows) of the 10 cases (1998-2005) studied; the base map is the July/August averaged TRMM sea surface temperature map of the same period; locations of the pre-cyclone Argos in situ profiles taken inside and outside of the intensification zone are depicted as stars and triangles, respectively. The location of the in situ profile found within 24h from Supertyphoon Dianmu's passage is depicted as square.

Corresponding author: Dr. I-I Lin, Dept. of Atmospheric Sciences, National Taiwan University, No. 1, Sec. 4, Roosevelt Rd., Taipei 106, Taiwan; e-mail: iilin@webmail.as.ntu.edu.tw

¹ Based on the best track data from the US Navy's Joint Typhoon Warning Center.

Why these super cyclones only intensify in this specific area of the ocean? For decades investigation has been hindered by the lack of information in this remote region due to difficulties in conducting ship-based observations at or near super typhoons. Recent advancement in the deployment of Argo ocean *in situ* floats (Gould et al., 2004) and satellite remote sensing, including QuikSCAT ocean surface wind vector (Liu et al., 1998), TRMM cloud-penetrating sea surface temperature (Wentz et al., 2000), and sea surface height anomaly from TOPEX/Poseidon and JASON-1 (Fu et al., 1994), provides new opportunities to look into this issue. Searching through the entire database, we use all the 10 available super cyclone cases², extending across 8 years (1998-2005), to show observational evidences on the unique relation between the super cyclone intensification and the underlying oceanic thermal structure. This information is also used as input in numerical experiments to explain this long-specified geographical dependence.

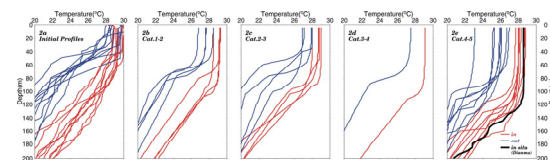
IS SEA SURFACE TEMPERATURE THE ONLY ANSWER?

Fig. 1b depicts the tracks of the cyclone cases studied in this work; track segments of intensification (from category-1 to 5) are shown in black and the base map is the averaged summer TRMM (Wentz et al., 2000) satellite sea surface temperature (SST) since 1998. Locations of the Argo (Gould et al., 2004) *in situ* ocean depth-temperature profiles inside and outside of the intensification zone (green box) are marked with stars and triangles, respectively (Fig. 1b). One would then ask which oceanic attribute is responsible for such geographical dependence? Warm pre-cyclone sea surface temperature is naturally the first candidate to be considered (Emanuel, 2000b, Free et al., 2004). As indicated in Fig. 1b, however, the warm summer SST of 28-30° C extends well beyond the zone, stretching northward till 30° N and westward till 100° E in the South China Sea. Why don't we observe the intensification of super cyclones in the South China Sea, for example, while its summer SST is equally warm? This shows that the warm SST argument alone can't conclusively explain the observed geographical dependence, and suggests other

² The 10 super cyclone cases are: Zeb (1998), Bilis (2000), Saomai (2000), Fengshen (2002), Hagibis (2002), Maemi (2003), Dianmu (2004), Chaba (2004), Haitang (2005), and Nabi (2005).

factor in affecting the location of the super-cyclone intensification zone.

In search for other factors, we compare the pre-cyclone *in situ* ocean depth-temperature profiles³ acquired inside and outside of the intensification zone. Clear distinction is found in the sub-surface temperature structure, but not in the sea surface temperature (Fig. 2a). Inside the intensification zone (red profiles), extraordinarily thick layer (90-150m) of warm water ($\geq 26^\circ$ C) is found; while outside the intensification zone (blue profiles) the warm water only extends to about 30-50m (Fig. 2a). This implies that the intensification zone is probably associated with the presence of the thick, warm sub-surface ocean temperature structure. To further explore this idea, we conduct a series of numerical experiments⁴ using an ocean mixed layer model (Price et al., 1986) with the observed warm sub-surface structure (red profiles in Fig. 2a) as input. Comparison experiments are also conducted using the reference profiles (blue profiles in Fig. 2a) outside the intensification zone. These experiments simulate ocean's dynamic response to cyclone's wind forcing because the strong wind of cyclone can mix the cold water from the deeper ocean layer to the warm upper layer and causes cooling (Price, 1981). This self-induced cooling response needs to be studied as it plays a critical negative feedback role in cyclone's intensification (Emanuel, 1999; Bender and Ginis, 2000; Cione and Uhlhorn, 2003).



³ For each super cyclone case, two Argo *in situ* profiles, one inside and one outside of the intensification zone, are chosen. All profiles are acquired between 1-9 days prior to super cyclone's passage. All inside profiles are acquired between 0.5 to 2 degrees from the storm tracks.

⁴ For each case, the mixed layer model is forced by the QuikSCAT ocean surface wind vectors under subsequent stages of intensification. In the model, the upper ocean thermal structure is initialized by the pre-cyclone Argo *in situ* profiles. Similar set of experiments using the reference profiles outside the intensification zone is also conducted for comparison. Due to the availability of the QuikSCAT wind vector data, experiments are conducted for 4 cases under intensification stage from category 1-2, 4 cases from category 2-3, 1 case from category 3-4, and 8 cases from category 4-5.

Figure 2: (a) Pre-cyclone ARGO *in situ* ocean depth-temperature profiles of the 10 super cyclone cases, profiles inside and outside of the intensification zone are depicted in red and blue, respectively. (b)-(e) Mixed-layer model simulated depth-temperature profiles under subsequent intensification stages⁴. The *in situ* profile found within 24h from Supertyphoon Dianmu's passage is depicted in black in (e); its location is depicted as square in Figs. 1b and 3.

OCEAN SUB-SURFACE STRUCTURE AND SUPER CYCLONE'S INTENSIFICATION

Table 1 and Figs. 2b-2e summarise the model results. With the temperature profiles from those inside the zone, the self-induced cooling remains little for all cases and increases only gradually (0.4 to 1.0 °C) in response to the intensification of tropical cyclone and the enhanced mixing effect. Even at the final intensification stage (from category-4 to 5, Fig. 2e) when the mixing depth reaches as deep as 120m (Table 1a, red profiles in Fig. 2e), the self-induced cooling is still limited to 1.0 ± 0.4 °C. The above result shows that the thick, warm sub-surface structure is robust enough to limit the self-induced cooling even under intense winds. This situation can be independently verified by the *in situ* profile (black profile in Fig. 2e) found within 24h from Supertyphoon Dianmu's passage of the intensification zone. On the contrary, the cooling outside the intensification zone is profound and increases rapidly (from 1.3 to 3.1 °C) with cyclone's intensification and enhanced mixing (Table 1b, blue profiles in Figs. 2b-2e).

	Cat. 1-2	Cat. 2-3	Cat. 3-4	Cat. 4-5
(a). inside	0.4±0.3	0.5±0.6	0.3±0.0	1.0±0.4
(b). outside	1.3±1.0	1.7±1.4	1.3±0.0	3.1±0.9

Table 1: Averaged model-estimated self-induced cooling (in °C) at each stage of the intensification; (a): profiles inside the intensification zone, (b): for reference profiles outside the intensification zone. Cooling exceeding 2.5 °C are highlighted in red, indicating unfavorable condition for intensification (Emanuel, 1999; Cione et al., 2003).

What is the implication of these cooling trends on typhoon's intensification? From Emanuel (1999), a mere 2.5 °C cooling is sufficient to shut down the entire energy production of tropical cyclones; rendering the effect of the cyclones' self-induced cooling a very efficient 'intensi-stat' (an intensity controller analogous to a thermo-stat which controls temperature). It can be seen in Table 1 that outside the zone, the cooling of 3.1 °C exceeds the threshold value of 2.5 °C during the intensification stage from category 4 (1-minute averaged wind

speed 114-135 kt) to 5, showing a highly unfavourable condition for intensification to the category-5 intensity. Whereas within the intensification zone, the cooling is well-confined to 1.0 °C or less, showing no restraint for cyclone from being boosted all the way up to the super category-5 scale.

BOOSTERS WHICH FUEL THE XTRAORDINARY INTENSITY OF SUPER CYCLONES

Finally, tracing back the oceanographic origin of the intensification zone, we see two different causes. The southern part of the zone (121-170° E, 9-20° N) is located at the thickest belt of the warm subtropical gyre. As illustrated in Fig. 3 that in this part of the gyre, the depth of the 26 °C isotherm (Stephens et al., 2001) can reach as deep as 80-130m, consistent with the observed structure (red profiles) shown in Fig. 2a. At the northern part the zone (121-170° E, 20-25° N), warm ocean eddies are the cause. Though the prevailing warm water at the northern section is not as thick (i.e., 26 °C isotherm at 30-70m, Fig. 3) as in the southern section, this region is known to have frequent occurrence of warm ocean eddies (Qiu, 1999) and the presence of warm ocean eddy can effectively deepen the warm water. By using the satellite sea surface height anomaly data, we found that the two supertyphoons (Maemi and Saomai) occurring in the northern section were indeed riding on two prominent warm ocean eddies. Using sea surface height anomaly data, we re-generate the 26 °C isotherm in these two eddies (Shay et al., 2000). As illustrated in Fig. 3, the 26 °C isotherm can reach as deep as 140m for Maemi and 100m for the Saomai case, therefore consistent with the observed structure (red profiles) in Fig. 2a. The above finding is further verified by a series of numerical experiments using the Coupled Hurricane Intensity Prediction System (Emanuel, et al., 2004) that Supertyphoon Maemi could not have reached the category-5 intensity without the presence of the warm ocean eddy (Lin et al., 2005).

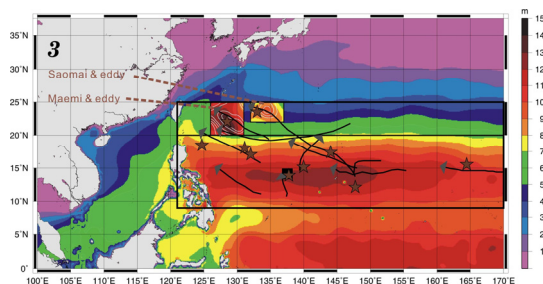


Figure 3: The May-October averaged climatological map (Stephens et al., 2002) of the 26 °C isotherm

in the Northwest Pacific Ocean with the regenerated (using satellite sea surface height anomaly data, as in Shay et al., 2000) 26 ° C isotherm at the 2 warm ocean eddy regions. Note the intensification zone is delimited as the southern (121-170 ° E, 9-20 ° N) and northern parts (121-170 ° E, 20-25 ° N).

In summary, both the thick, warm gyre belt and warm ocean eddies are necessary boosters for the super cyclones in the Northwest Pacific Ocean. On these boosters, tropical cyclones can intensify without being constrained by the self-induced cooling and reach the super, category-5 intensity. This work highlights the critical role of ocean sub-surface structure in controlling the presence of super cyclones. Identifying boosters in other ocean basins (e.g., the Atlantic and the Eastern Pacific Ocean) is imperative, given the recent devastation of Hurricane Katrina to the Gulf States of USA. The impact from this ocean sub-surface thermal structure on the tropical cyclone intensity also has to be carefully addressed when the impact of climate change on tropical cyclone intensity is assessed (Emanuel, 2005; Webster, et al., 2005).

References

- Bender, M. A., and I. Ginis, 2000: Real-case simulations of hurricane-ocean interaction using a high-resolution coupled model: effects on hurricane intensity. *Mon. Wea. Rev.*, **128**, 917-946.
- Bosart, L. F., C. S. Velden, W. E. Bracken, J. Molinari, and P. G. Black, 2000: Environmental Influences on the Rapid Intensification of Hurricane Opal (1995) over the Gulf of Mexico. *Mon. Wea. Rev.*, **128**, 322-352.
- Cione, J. J., and E. W. Uhlhorn, 2003: Sea surface temperature variability in hurricanes: Implications with respect to intensity change. *Mon. Wea. Rev.*, **131**, 1783-1796.
- Emanuel, K., 1999: Thermodynamic control of hurricane intensity. *Nature*, **401**, 665-669.
- Emanuel, K. A., 2000a: A similarity hypothesis for air-sea exchange at extreme wind speeds. *J. Atmos. Sci.* **60**, 1420-1428.
- Emanuel, K. A., 2000b: A statistical analysis of tropical cyclone intensity. *Mon. Weath. Rev.* **128**, 1139-1152.
- Emanuel, K. A., C. DesAutels, C. Holloway C., and R. Korty, 2004: Environmental control of tropical cyclone intensity. *J. Atmos. Sci.* **61**, 843-858.
- Emanuel, K. A., 2005: Increasing destructiveness of tropical cyclones over the past 30 years. *Nature* **436**, 686-688.
- Free, M., M. Bister M., K. Emanuel, 2004: Potential intensity of tropical cyclones: Comparison of results from radiosonde and reanalysis data. *J. Clim.* **17**, 1722-1727.
- Fu, L. L., E. J. Christensen, C. A. Yamarone, M. Lefebvre, Y. Menard, M. Dorrer, and P. Escudier, 1994: TOPEX/POSEIDON Mission Overview. *J. Geophys. Res.* **99**, 24369-24381.
- Goni, G. J., and J. A. Trinanes, 2003: Ocean thermal structure monitoring could aid in the intensity forecast of tropical cyclones. *Eos, Trans. Amer. Geophys. Union*, **84**, 573-580.
- Gould, J., D. Roemmich, S. Wijffels, H. Freeland, M. Ignaszewsky, X. Jianping, S. Pouliquen, Y. Desaubies, U. Send, K. Radhakrishnan, K. Takeuchi, K. Kim, M. Danchenkov, P. Sutton, B. King, B. Owens, and S. Riser, 2004: Argo profiling floats bring new era of *in situ* ocean observations. *Eos, Trans. Amer. Geophys. Union*, **85**, 179, 190-191.
- Holliday, R.H., and A. H. Thompson, 1979: Climatological characteristics of rapidly intensifying typhoons. *Mon. Weath. Rev.* **107**, 1022-1034.
- Lin, I-I, C.-C. Wu, K. A. Emanuel, I.-H. Lee, C.-R. Wu, and I.-F. Pun, 2005: The interaction of supertyphoon Maemi with a warm ocean eddy. *Mon. Weath. Rev.*, **133**, 2635-2649.
- Liu, W.T., W. Tang, and P. S. Polito, 1998: NASA Scatterometer provides global ocean-surface wind fields with more structures than numerical weather prediction. *Geophys. Res. Lett.* **25**, 761-764.
- Price, J.F., 1981: Upper ocean response to a hurricane. *J. Phys. Oceanogr.* **11**, 153-175.
- Price, J.F., R. A. Weller, R.A., and R. Pinkel, 1986: Diurnal cycling: observations and models of the upper ocean response to diurnal heating, cooling, and wind mixing. *J. Geophys. Res.* **91**, 8411-8427.
- Qiu, B., 1999: Seasonal eddy field modulation of the North Pacific Subtropical Countercurrent: TOPEX/Poseidon observations and theory. *J. Phys. Oceanogr.* **29**, 1670-1685.
- Shay, L. K., G. J. Goni, and P. G. Black, 2000: Effects of a warm oceanic feature on Hurricane Opal. *Mon. Weath. Rev.* **128**, 1366-1383.
- Stephens, C., J. I. Antonov, T. P. Boyer, M. E. Conkright, R. Locarnini, and T. D. O'Brien, 2002: World ocean atlas 2001 Volume 1: temperature [CD-ROM], edited by S. Levitus, NOAA Atlas NESDIS 49, U.S. Govt. Printing Office, Washington, D.C.

- Wang, Y., and C. C. Wu, 2004: Current understanding of tropical cyclone structure and intensity changes – a review. *Meteorol. Atmos. Phys.* **87**, 257-278.
- Webster, P. J., G. J. Holland, J. A. Curry, and H.-R. Chang, 2005: Changes in tropical cyclone number, duration, and intensity in a warming environment. *Science*, **309**, 1844-1846.
- Wentz, F.J., C., Gentemann, D., Smith, and D., Chelton, 2000: Satellite measurements of sea surface temperature through clouds. *Science*. **288**, 847-850.

Acknowledgements

We thank Dr. Colin Stark for his helpful comments and Prof. Dong-Ping Wang for providing the mixed layer model. Thanks also to NASA, Remote Sensing Systems, Argo *in situ* ocean float team, and the Joint Typhoon Warning Center for data provision. This work is supported by the National Science Council, Taiwan through NSC 94-2119-M-002-019-AP1, NSC 93-2119-M-002-013-AP1, and NSC93-2119-M-002-010-AP1.